

Research Paper

The Ca^{2+} release-activated Ca^{2+} current (I_{CRAC}) mediates store-operated Ca^{2+} entry in rat microglia

Lily Ohana,^{1,†} Evan W. Newell,^{1,2,†,‡} Elise F. Stanley^{1,2} and Lyanne C. Schlichter^{1,2,*}

¹Toronto Western Research Institute; University Health Network; ²Department of Physiology; University of Toronto; Toronto, ON CA

[‡]Current address: Department of Microbiology and Immunology; Stanford University; Stanford, CA USA

[†]These authors contributed equally to this work.

Abbreviations: 2-APB, 2-aminoethoxydiphenyl borate; CR3, complement receptor 3; CRAC, Ca^{2+} -release activated Ca^{2+} ; DES, diethylstilbestrol; DVF, divalent-free; FBS, fetal bovine serum; HEDTA, N-(2-hydroxyethyl)ethylenediamine-N,N',N'-triacetic acid; HPRT1, hypoxanthine guanine phosphoribosyl transferase; KCa, Ca^{2+} -activated K^+ channel; Kir, inward-rectifier potassium channel; K_v , voltage-gated delayed rectifier potassium channel; LPS, lipopolysaccharide; NMDG, N-methyl-D-glucamine; SOCE, store-operated Ca^{2+} entry; SOC, store-operated channel; STIM-1, stromal interaction molecule 1; TRP, transient receptor potential; V_m , membrane potential

Key words: calcium signaling, brain macrophages, SOCE

Ca^{2+} signaling plays a central role in microglial activation, and several studies have demonstrated a store-operated Ca^{2+} entry (SOCE) pathway to supply this ion. Due to the rapid pace of discovery of novel Ca^{2+} permeable channels, and limited electrophysiological analyses of Ca^{2+} currents in microglia, characterization of the SOCE channels remains incomplete. At present, the prime candidates are 'transient receptor potential' (TRP) channels and the recently cloned Orai1, which produces a Ca^{2+} -release-activated Ca^{2+} (CRAC) current. We used cultured rat microglia and real-time RT-PCR to compare expression levels of Orai1, Orai2, Orai3, TRPM2, TRPM7, TRPC1, TRPC2, TRPC3, TRPC4, TRPC5, TRPC6 and TRPC7 channel genes. Next, we used Fura-2 imaging to identify a store-operated Ca^{2+} entry pathway that was reduced by depolarization and blocked by Gd^{3+} , SKF-96365, diethylstilbestrol (DES), and a high concentration of 2-aminoethoxydiphenyl borate (50 μM 2-APB). The Fura-2 signal was increased by hyperpolarization, and by a low concentration of 2-APB (5 μM), and exhibited Ca^{2+} -dependent potentiation. These properties are entirely consistent with Orai1/CRAC, rather than any known TRP channel and this conclusion was supported by patch-clamp electrophysiological analysis. We identified a store-operated Ca^{2+} current with the same properties, including high selectivity for Ca^{2+} over monovalent cations, pronounced inward rectification and a very positive reversal potential, Ca^{2+} -dependent current potentiation, and

block by SKF-96365, DES and 50 μM 2-APB. Determining the contribution of Orai1/CRAC in different cell types is crucial to future mechanistic and therapeutic studies; this comprehensive multi-strategy analysis demonstrates that Orai1/CRAC channels are responsible for SOCE in primary microglia.

Introduction

In response to central nervous system (CNS) damage or disease, microglia undergo complex responses, often collectively called 'activation'. This can result in upregulation of functions that involve Ca^{2+} signaling: proliferation, migration, phagocytosis, and production of nitric oxide, interleukins, cytokines and chemokines (reviewed in refs. 1–7). More than 20 receptor/ligand interactions have been reported to elevate Ca^{2+}_i in microglia, and Ca^{2+} entry can be mediated by ionotropic purinergic receptors, reversed $\text{Na}^+/\text{Ca}^{2+}$ exchange,⁸ and store-operated Ca^{2+} entry (SOCE) (reviewed in refs. 9–11). SOCE serves as a central pathway for Ca^{2+} signaling in non-excitabile cells¹² and, in microglia, numerous receptor-mediated responses evoke Ca^{2+} release from intracellular stores, followed by SOCE. The resulting Ca^{2+} rise that lasts for minutes to hours can immediately affect activity of Ca^{2+} -dependent proteins, such as calmodulin and Ca^{2+} -activated K^+ channels,¹³ and help replenish intracellular Ca^{2+} stores, but it can also have long-term effects on gene expression and cell cycle regulation (reviewed in refs. 10 and 12).

There is little electrophysiological information about the identity of the underlying Ca^{2+} -permeable channel(s) in microglia, despite numerous studies using Ca^{2+} -sensitive dyes to investigate receptor-mediated signals. The literature on other cell types suggests that SOCE can be conferred by multiple channel types, collectively called store-operated channels (SOCs), but whose molecular identities are contentious (see Discussion). A subtype

*Correspondence to: Lyanne C. Schlichter; Toronto Western Research Institute; 399 Bathurst Street; Toronto, ON MC9-417 Canada; Tel.: 416.603.5970; Fax: 416.603.5745; Email: schlicht@uhnres.utoronto.ca

Submitted: 02/13/09; Revised: 03/31/09; Accepted: 04/02/09

Previously published online as a *Channels* E-publication:

<http://www.landesbioscience.com/journals/channels/article/8609>

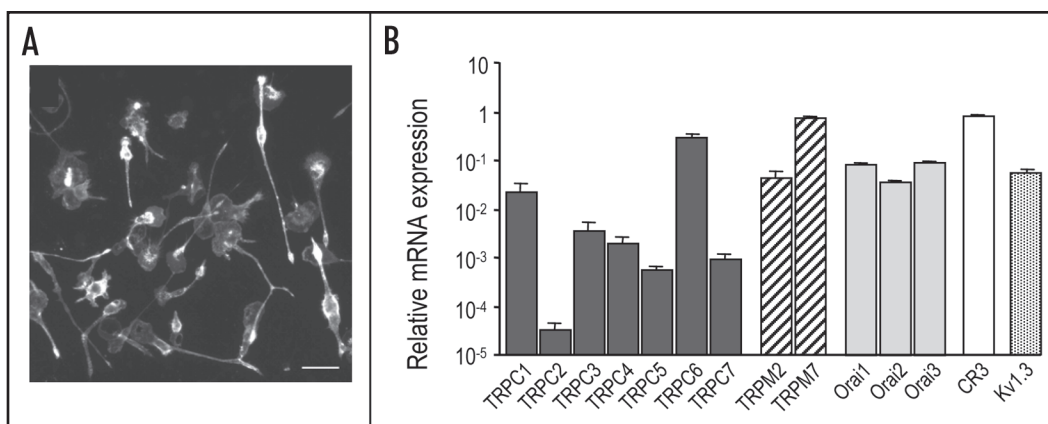


Figure 1. Expression of TRP and Orai channels in rat microglia. (A) The microglia cultures were essentially pure (99–100%), as judged by labeling with FITC-conjugated tomato lectin. Scale bar, 50 μ m. (B) Relative mRNA expression was monitored by quantitative real-time RT-PCR (qRT-PCR), standardized to the housekeeping gene, HPRT-1 (see Materials and Methods). Values shown are mean \pm SEM from 4 mRNA preparations made from separate batches of microglia isolated from different rat litters.

of SOC with specific electrophysiological properties was first characterized in mast cells and immune cell lines and called the Ca²⁺-release activated Ca²⁺ (CRAC) channel¹⁴ (reviewed in ref. 15). The molecular identity of CRAC also remained elusive for many years, until the cloning of Orai1/CRACM^{16,17} and evidence it contributes to the pore-forming unit.^{18,19} Importantly, with recent molecular, biophysical and pharmacological fingerprinting, the CRAC current has been better defined, and a clearer distinction made from other SOC currents. Three patch clamp studies have addressed store-operated and CRAC currents in microglia^{20–22} and each has provided valuable information. The earlier studies were done before several fundamental properties of Orai1/CRAC had been elucidated and, as addressed in the Discussion, it is crucial to consolidate and extend these studies using the latest criteria for distinguishing Orai/CRAC from other co-existing current in microglia. Hence, we have combined Ca²⁺ imaging, patch-clamp recordings and pharmacological approaches to study SOCE and the underlying currents in primary cultures of rat microglia.

Results

Expression of putative Ca²⁺-permeable channels in rat microglia. Quantitative real-time RT-PCR (qRT-PCR) was used to compare mRNA expression levels of Ca²⁺-permeable channels in cultured microglia (Fig. 1A); including the main candidate genes for store operated Ca²⁺ channels (Fig. 1B). Transcripts for several 'transient receptor potential' (TRP) genes were detected. Quantitative comparisons of mRNA expression showed that TRPM7 > TRPC6 > TRPM2 > TRPC1 > TRPC3 \geq TRPC4 > TRPC7 > TRPC5 > TRPC2, where '>' denotes a significant difference ($p < 0.05$) from the preceding gene, and ' \geq ' indicates a non-significant difference (one way ANOVA, followed by Tukey's test for multiple comparisons). Note that mRNA expression for TRPM7 and for the microglial marker, complement receptor 3 (CR3), was high and comparable to the housekeeping gene, HPRT-1. Relatively high mRNA levels were seen for the recently cloned Orai genes (Orai3 \geq Orai1 > Orai2), which

were more abundant than TRPC genes, except for TRPC6. Orai expression levels were similar to the most commonly studied ion channel in microglia, voltage gated delayed rectifier potassium channel, K_v1.3, which contributes to microglial proliferation and activation.^{23,34}

Properties of store-operated Ca²⁺ entry (SOCE) in rat microglia. Having detected mRNA expression for several candidates for Ca²⁺ release activated Ca²⁺ (CRAC/Orai) channels and other SOCs; we next examined store-operated Ca²⁺ entry. In microglia loaded with Fura-2AM in the standard bath solution containing 1 mM Ca²⁺, intracellular Ca²⁺ (Ca²⁺_i) was low (23 \pm 2 nM; $n = 99$ cells), and there was little change upon removal of extracellular Ca²⁺ (nominally Ca²⁺-free, 0 Ca) (Fig. 2A). Depleting the stores with thapsigargin (1 μ M) evoked a small Ca²⁺ transient that varied in size and kinetics (Figures show average responses from several cells). Then, when external Ca²⁺ (Ca²⁺_o) was restored to 1 mM, Ca²⁺ rebound increased Ca²⁺_i within seconds, reaching 170 \pm 9 nM after one minute. A similar response was seen in all cells examined; i.e., >500 cells from 12 separate cell cultures, clearly demonstrating SOCE. In control recordings without drugs or solution changes (not shown), the Ca²⁺_i signal spontaneously declined to a plateau in the continued presence of external Ca²⁺; decreasing to 50% from the peak value in 54 \pm 26 sec ($n = 58$ cells from three separate cultures).

As a first step toward determining which of the expressed channels is involved in the SOCE (Orai/CRAC or another SOC), we examined its pharmacological properties (Fig. 2), using the well known SOCE inhibitors, SKF-96365 and Gd³⁺,^{12,15} as well as diethylstilbestrol (DES)³⁵ and 2-aminoethoxydiphenyl borate (2-APB).^{12,36} When thapsigargin was added in a Ca²⁺-free bath solution and SOCE was evoked by restoring external Ca²⁺ (Fig. 2A), 10 μ M DES nearly abolished the Ca²⁺_i rise. Similarly, when SOCE was triggered by restoring Ca²⁺_o after pre-incubation with thapsigargin in a Ca²⁺-free bath solution (Fig. 2B); it was decreased by SKF-96365 and Gd³⁺. An important pharmacological discrimination was then based on 2-APB, which blocks some TRP

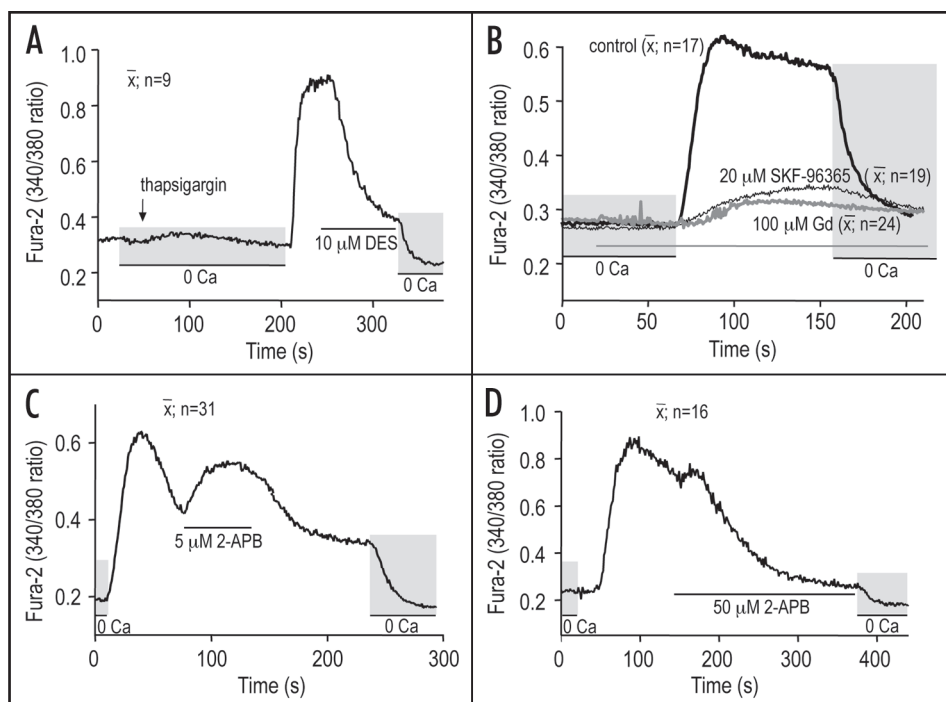


Figure 2. Properties of store-operated Ca^{2+} entry (SOCE) in rat microglia. The average intracellular Ca^{2+} was monitored in groups of microglia loaded with Fura-2AM in standard bath solution (A) or in a nominally Ca^{2+} free bath solution, which contained $1 \mu\text{M}$ thapsigargin for (B–D). For clarity, periods in Ca^{2+} free bath solution are shown by grey boxes, and perfusion with pharmacological agents is indicated by horizontal lines. (A) Inhibition of SOCE by $10 \mu\text{M}$ diethylstilbestrol (DES). SOCE was evoked by adding $1 \mu\text{M}$ thapsigargin in Ca^{2+} free bath solution and then restoring external Ca^{2+} . (B) Inhibition of SOCE by $20 \mu\text{M}$ SKF-96365 or $100 \mu\text{M}$ Gd^{3+} added to separate cell batches during the period indicated by the grey line. (C) Increase in SOCE by $5 \mu\text{M}$ 2-aminoethoxydiphenyl borate (2-APB); same protocol as in (B). (D) Inhibition of SOCE by $50 \mu\text{M}$ 2-APB.

channels, but exerts a dual effect on CRAC—increasing it at low concentrations ($1\text{--}5 \mu\text{M}$) and blocking it at higher concentrations (e.g., $40\text{--}50 \mu\text{M}$).³⁶ After evoking SOCE as in panel B, perfusing in $5 \mu\text{M}$ 2-APB (Fig. 2C) evoked a substantial increase in Ca^{2+}_i (as expected for CRAC), and this was reversed upon drug washout. The higher 2-APB concentration ($50 \mu\text{M}$; Fig. 2D) evoked a small increase just as the drug began to enter the bath, and then the Ca^{2+}_i rise was essentially abolished. Block by these four compounds and the dual effect of 2-APB provides evidence that CRAC channels mediate this SOCE in microglia.

Further characterization was based on the effect of membrane potential on SOCE. We have previously shown that both K^+ and Cl^- channels contribute to the membrane potential (V_m) of rat microglia, and that 55 mM external K^+ depolarizes the cells to about -15 mV .²⁴ In Figure 3A, cells were loaded with Fura-2 in 1 mM external Ca^{2+} , and then thapsigargin was added to evoke Ca^{2+} release from stores, followed by SOCE. When external K^+ was elevated, the sustained Ca^{2+}_i plateau decreased, and then rebounded when normal external K^+ was restored and, as in Figure 2B, the SOCE was inhibited by Gd^{3+} . [Note: this response is opposite to our recently described contribution of reversed $\text{Na}^+/\text{Ca}^{2+}$ exchanger activity, seen in a small proportion of microglia⁸]. Next, the contribution of V_m was directly examined by imaging

Fura-2 during perforated-patch recordings with amphotericin (Fig. 3B). This method allows whole-cell recording by forming channels that are permeable to small monovalent ions but impermeable to divalent cations,³⁷ such that Ca^{2+}_i responses are not compromised. Intracellular Ca^{2+} stores were first depleted using thapsigargin in a Ca^{2+} -free solution, and then SOCE was evoked by perfusing in 1 mM Ca^{2+} (as in Fig. 2). The Ca^{2+}_i response was compared in each microscope field between several intact microglia and a single patch-clamped cell whose membrane potential was held at -50 mV to reflect the normal resting potential, which we previously measured with voltage-sensitive dyes.²⁴ SOCE was decreased by depolarizing V_m to -10 mV and increased by hyperpolarizing to -90 mV (Fig. 3B). Similar results were seen in eight different fields of microglial cells, consistent with depolarization reducing the driving force for Ca^{2+} entry. Cells whose V_m was not controlled by patch clamping (dashed curve) showed the typical monotonic Ca^{2+}_i rise that occurs when external Ca^{2+} is restored to store-depleted cells.

Ca^{2+} -dependent potentiation of SOCE as evidence for CRAC channels.

A biophysical property that helps distinguish Orai/CRAC from TRP channels is that the CRAC current displays Ca^{2+} -dependent potentiation; i.e., an increase in inward current as Ca^{2+} enters.^{12,14,38} Ca^{2+} -dependent potentiation is more pronounced with hyperpolarization (less Ca^{2+} enters at depolarized potentials)^{12,15} and it is not supported by Ba^{2+} or Sr^{2+} .³⁹ Such ion substitutions are useful because several TRPC channels (TRPC1, C4, C5, C6) are permeable to Ba^{2+} ,⁴⁰⁻⁴³ but do not display Ca^{2+} -dependent potentiation. Ba^{2+} and Sr^{2+} influx can be detected by Fura-2 imaging,⁴⁴ thus, we compared Fura-2 signals when Ca^{2+}_o was replaced with either of these divalent cations. In microglia that were exposed to a Ca^{2+} -free bath solution (without thapsigargin), there was no Ca^{2+} rebound when 1 mM Ca^{2+} was restored, nor was there a response to a brief exposure to 1 mM Sr^{2+} (Fig. 4A). When thapsigargin was added, Ca^{2+} release evoked only a transient Fura-2 signal that returned to baseline as the stores were depleted (see Materials and Methods for Fura-2 K_d 's and calculations). Re-exposure to 1 mM Sr^{2+} did not elicit a Fura-2 signal; however, thapsigargin had activated the SOCE, as seen by the large Fura-2 signal evoked by restoring Ca^{2+}_o . This signal immediately decreased when Ca^{2+} was again replaced by Sr^{2+} . This result is consistent with Sr^{2+} neither evoking nor sustaining a previously activated SOCE. An alternative explanation, that the Sr^{2+} permeability is too low, is

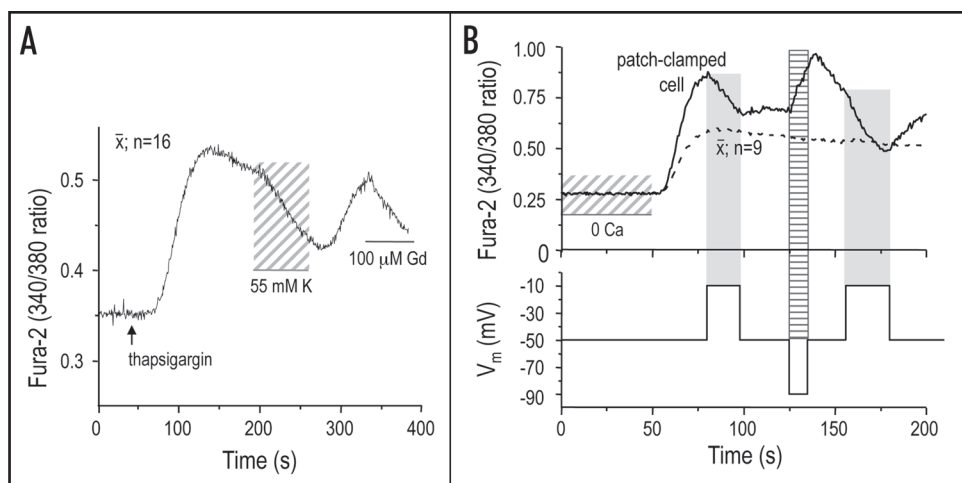


Figure 3. Voltage dependence of SOCE. (A) Cells were loaded with Fura-2 in standard bath solution and exposed to 1 μM thapsigargin, as indicated. During the plateau phase of the Ca^{2+} rise, the bath was perfused with a depolarizing solution in which 50 mM Na^+ was replaced with K^+ (55 mM total K^+), and then with standard solution. Finally, 100 μM Gd^{3+} was added to the bath. (B) Intracellular Ca^{2+} was monitored in a microscope field containing ten Fura-2 loaded microglia, while one cell was voltage-clamped in the perforated-patch mode using amphotericin (see Materials and Methods). For clarity, Ca^{2+} responses to depolarizing voltages are shown by solid grey bars, and a hyperpolarizing change is shown by the dashed bar. Cells were loaded with Fura-2AM in Ca^{2+} free bath solution containing 1 μM thapsigargin to deplete intracellular Ca^{2+} stores. From a holding potential of -50 mV, voltage-clamp steps were made to -10, -50 and -90 mV to monitor the Ca^{2+} signal in the voltage-clamped cell (solid trace). The average Ca^{2+} response is shown for the remaining cells in the field (dashed trace).

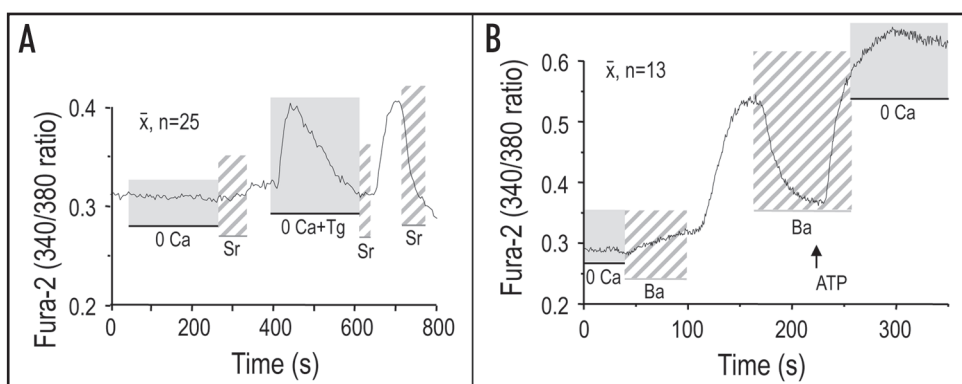


Figure 4. Ca^{2+} -dependent potentiation of SOCE as evidence for CRAC channels. (A) Ca^{2+} imaging of microglia that were loaded with Fura-2AM in standard bath solution. The grey bars indicate periods when the standard bath solution was replaced with Ca^{2+} -free solution (0 Ca). The dashed bars show periods when 1 mM Sr^{2+} (Sr) replaced the external Ca^{2+} ; Tg, addition of 1 μM thapsigargin. (B) Effects of external Ba^{2+} on the SOCE in microglia that had been loaded with Fura-2AM in Ca^{2+} -free bath solution containing 1 μM thapsigargin. Grey bars, Ca^{2+} free solution (0 Ca); dashed bars show periods when 1 mM Ba^{2+} (Ba) replaced the external Ca^{2+} . The arrow shows when 100 μM ATP was added to the bath.

unlikely because immediately after their activation, Orai/CRAC channels and other SOC channels support more Sr^{2+} and Ba^{2+} influx than Ca^{2+} .^{12,15,39} These data provide further evidence that Orai/CRAC channels mediate the SOCE.

The effects of Ba^{2+} substitution for external Ca^{2+} provide further evidence that the SOCE is mediated by CRAC channels. In cells pre-incubated with thapsigargin in a Ca^{2+} -free bath

solution, cytoplasmic Ca^{2+} was 20.2 nM, as calculated from the initial Fura-2 ratio (0.29 ± 0.002 ; $n = 53$ cells). Depletion of intracellular Ca^{2+} is expected to prevent the Ca^{2+} -dependent potentiation of Orai/CRAC channels, if they are active. The first exposure to 1 mM Ba^{2+} (Fig. 4B) produced a small increase in the Fura-2 signal (in 53/60 cells), corresponding with 44 nM cytoplasmic Ba^{2+} ; at 60 s (Fura-2 ratio, 0.31 ± 0.004 ; see Materials and Methods for Fura-2 K_d 's and calculations). Then, restoring external Ca^{2+} evoked a substantial Fura-2 signal that increased over time to reach 133 nM Ca^{2+} at 60 s (Fura-2 ratio, 0.51 ± 0.01 ; $n = 38$ cells). The Fura-2 signal decreased substantially when Ba^{2+} was substituted for Ca^{2+} . Overall, these responses to Ba^{2+} are consistent with a lower Fura-2 response to Ba^{2+} (i.e., higher K_d ; see Materials and Methods) and with reversal of CRAC potentiation in the absence of Ca^{2+} influx. As a further control, we confirmed that Fura-2 responds to Ba^{2+} influx. That is, activation of the Ca^{2+} - and Ba^{2+} -permeable ionotropic purinergic P2X receptors⁴⁵ by 100 μM ATP produced a large Fura-2 signal with Ba^{2+} as the permeant ion, which corresponded with ~ 890 nM final Ba^{2+} . As expected, the Ba^{2+} signal remained elevated after its removal from the bath because the Ca^{2+} efflux pumps do not transport Ba^{2+} . After correcting for differences in the K_d of Fura-2 for binding Ca^{2+} (236 nM) versus Ba^{2+} (780 nM),³² the intracellular Ca^{2+} rise at 60 s was ~ 4 times higher than the Ba^{2+} rise. This is a conservative estimate because the reduced ability of cells to extrude Ba^{2+} compared to Ca^{2+} will underestimate the steady-state flux ratio. Our result is consistent with the 3–4 fold Ca^{2+} -dependent potentiation of CRAC current expected at -50 mV in 1 mM

external Ca^{2+} .⁴⁶ In addition, the relatively small Fura-2 signals with Sr^{2+} or Ba^{2+} are similar to CRAC-mediated Sr^{2+} and Ba^{2+} signals described previously, rather than the larger signals produced by TRPC channels.⁴⁴

Whole-cell recordings of the store-operated Ca^{2+} current in microglia. The pharmacological profile, divalent cation permeability and Ca^{2+} -dependent potentiation strongly support the notion

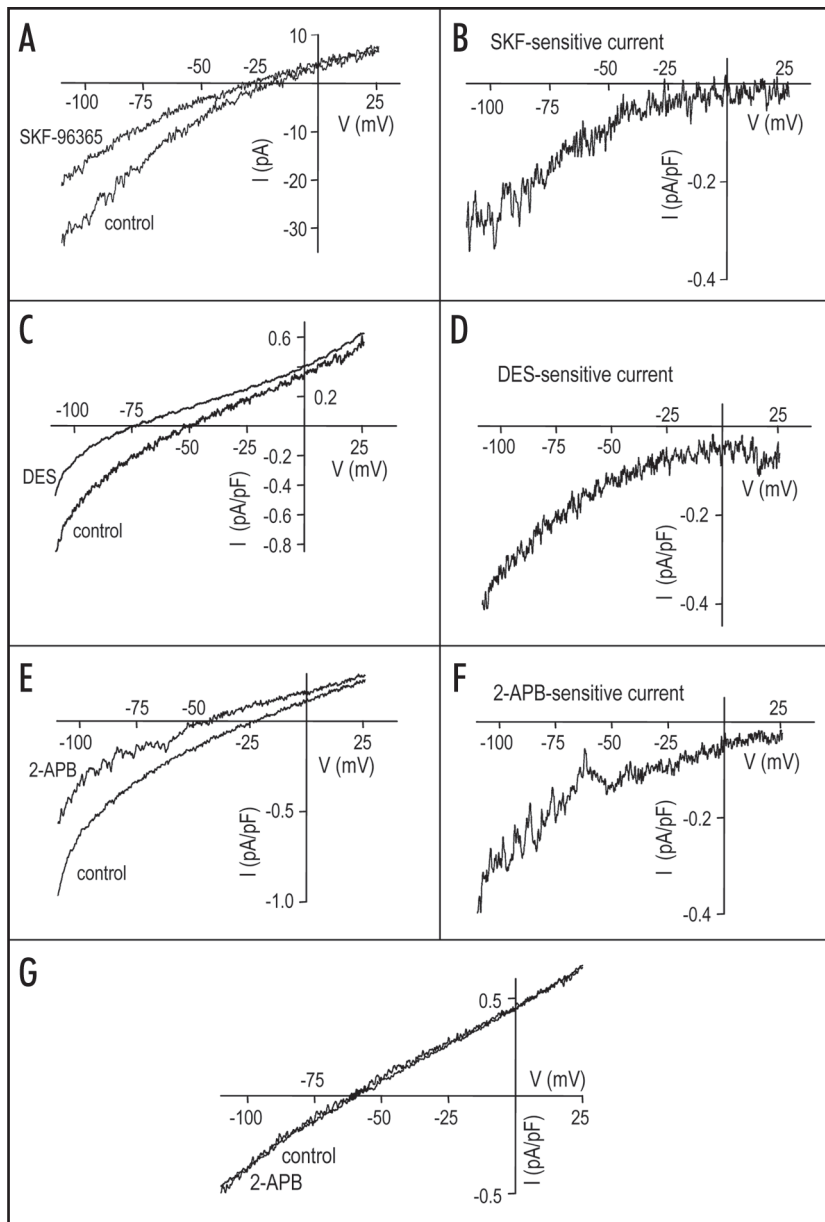


Figure 5. Isolation and pharmacology of the store-operated Ca^{2+} current in microglia. To activate store-operated Ca^{2+} currents, the pipette solution contained 10 mM BAPTA (20 nM free Ca^{2+}), and microglia were exposed to 1 μ M thapsigargin for 5–7 min in normal bath solution (A–F). Then, the bath was replaced with a K^+ free solution containing 10 mM Ca^{2+} and the whole-cell current-versus-voltage relation was monitored by applying voltage ramps (-110 to +25 mV) every 1 s from a holding potential of 0 mV. (A and B) A representative current-versus-voltage relation before (control) and after adding 20 μ M SKF-96365 (A). (B) shows isolation of the SKF-96365-sensitive current calculated as a point-by-point subtraction of the current in SKF-96365 from the control current. (C and D) Isolation of the diethylstilbestrol (DES)-sensitive current from a different cell using the same subtraction protocol as in (B and C), but before and after adding 10 μ M DES. (E and F) Isolation of the 2-aminoethoxydiphenyl borate (2-APB)-sensitive current from a different cell, using the same subtraction protocol, but before and after adding 50 μ M 2-APB. (G) Representative traces showing that the whole cell current in microglia without store depletion (no thapsigargin added) was not affected by 50 μ M 2-APB.

eliminating transmembrane osmotic gradients and by replacing almost all the internal Cl^- with the poorly permeant anion, aspartate.

To activate store-operated Ca^{2+} currents, we used low Ca^{2+} pipette solutions with strong Ca^{2+} buffering (10 mM BAPTA; 20 nM free Ca^{2+}) and then evoked depletion of the intracellular stores by bath applying 1 μ M thapsigargin. After 5–7 min the standard bath solution was replaced with a K^+ free bath solution containing elevated Ca^{2+} (10 mM); the store-activated Ca^{2+} current was isolated by subtraction of the component blocked by 20 μ M SKF-96365 (Fig. 5A and B). The example in Figure 5A shows total current in pA, while the other examples are presented as current density (pA/pF). The blocker-sensitive current component was inwardly rectifying and averaged 0.32 ± 0.03 pA/pF at -110 mV ($n = 3$). As expected, owing to lack of Cs^+ permeability through CRAC channels,¹² there was no outward current. Inward rectification and an extremely positive reversal potential are hallmarks of the highly Ca^{2+} selective currents mediated by CRAC and cloned Orai1 channels.^{12,51,52} In separate cells, the same subtraction protocol was used to examine two blockers shown above to inhibit the SOCE in microglia: 10 μ M DES (Fig. 5C and D), 50 μ M 2-APB (Fig. 5E and F). Each compound blocked an inwardly rectifying current of the same appearance and amplitude as the SKF-96365-sensitive component; i.e., 0.36 ± 0.01 pA/pF for DES, and 0.35 ± 0.01 pA/pF for 2-APB ($n = 3$ each). In a further test of specificity (Fig. 5G), the whole-cell current in microglia in which the store-operated Ca^{2+} current had not been activated (no thapsigargin) was not affected by 2-APB. This background current had a nearly linear current-versus-voltage relationship that reversed at about -60 mV, and thus was not a Ca^{2+} or cation non-selective

that the SOCE in microglia is mediated by Orai/CRAC channels. Thus, we used whole-cell patch-clamp recordings to isolate and characterize the store-operated Ca^{2+} currents. Key to the success of these experiments was finding ionic conditions that eliminated several potentially contaminating currents, as follows. All recordings were begun in standard bath solution, before any external ions were substituted. Then, Ca^{2+} currents were recorded using K^+ free external (and internal) solutions to avoid the K^+ currents we have observed in rat microglia under these culturing conditions; i.e., $K_V1.3$, inward-rectifier K^+ , Kir2.1, rat ether-a-go-go related gene (rERG) and Ca^{2+} -activated K^+ , $KCa3.1$.^{13,23,24,34,47-49} A high intracellular Mg^{2+} concentration (8 mM) was used to inhibit the TRPM7 current, which spontaneously activates within minutes after establishing whole cell recordings in rat microglia.⁵⁰ Inward anion currents e.g., swelling activated^{26,47} were minimized by

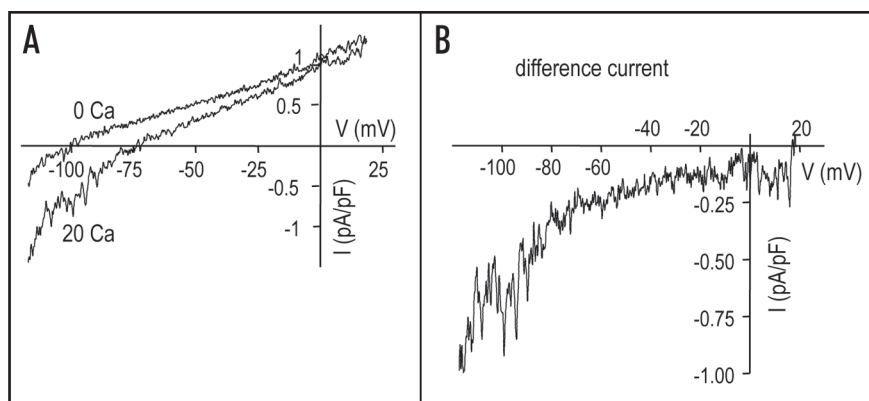


Figure 6. Isolation of the store-operated Ca^{2+} current in Na^+ free solutions. Microglia were incubated for 5–7 min with 1 μM thapsigargin, and then exposed to a NMDG⁺ bath solution without Ca^{2+} . The whole-cell current-versus-voltage (I-V) relation was continuously monitored by applying voltage ramps (-110 to +25 mV) every 1 s from a holding potential of 0 mV. (A) A representative I-V relation in NMDG⁺ bath solution without Ca^{2+} (0 Ca^{2+}) and after perfusing in a 20 mM Ca^{2+} bath solution. (B) Isolation of the Ca^{2+} current from the cell in (A), calculated by subtracting the current in 0 Ca^{2+} from that in 20 mM Ca^{2+} .

current. Variable levels of the background current produced a variable reversal potential of the total current in panels A, C and E.

The Ca^{2+} selectivity of the store-operated current was confirmed in cells in which the intracellular stores had been depleted using thapsigargin and strong intracellular Ca^{2+} buffering (Fig. 6). When Na^+ , K^+ and Ca^{2+} in the bath were replaced with the bulky cation, NMDG⁺, the small remaining current reversed at a very negative membrane potential (about -100 mV; Fig. 6A). Then, with 20 mM Ca^{2+} in the bath solution, the inward current increased and the reversal potential became less negative (about -75 mV). The difference current obtained from point-by-point subtraction was an inwardly rectifying current (Fig. 6B), with an average amplitude at -110 mV of 0.69 ± 0.06 pA/pF ($n = 3$).

Further evidence for a CRAC current: Ca^{2+} -dependent potentiation and pharmacology. Results from experiments illustrated in Figures 5 and 6 show an inwardly rectifying Ca^{2+} current activated after depletion of intracellular Ca^{2+} stores, and blocked by three known SOC channel inhibitors. However, because Orai1/CRAC and TRPC channels conduct Ca^{2+} , further experiments were needed to determine which channel most likely conducts the current. A hallmark of the CRAC current is the Ca^{2+} -dependent potentiation,¹² that was shown above using Fura-2 imaging of the SOCE. In whole-cell recordings, potentiation is usually demonstrated as a time-dependent decrease in current in Ca^{2+} free solution, superimposed on a tonic increase in monovalent cation current.⁵³ Hence, the stereotypical pattern upon removal of external divalent cations is a larger inward current with a rapid relaxation.^{14,54}

Evidence for Ca^{2+} -dependent potentiation of the store-operated current in microglia is presented in Figure 7. In panel A, the stores were depleted by thapsigargin in the standard bath solution containing 1 mM Ca^{2+} . Then, the bath was exchanged for a divalent-free (DVF) and K^+ -free solution with EDTA and HEDTA to eliminate any residual divalent cations (see Table 2).

After substituting DVF and K^+ -free bath solution there was a large inward current carried by Na^+ , which rapidly decayed as expected for CRAC. The inward current reached a plateau level, and then was nearly abolished after perfusing in the standard divalent-containing bath solution, as expected for channels with a very low conductance for Ca^{2+} . Adding 50 μM 2-APB greatly reduced the monovalent (Na^+) current in DVF solution, which then decayed to the same plateau level. The current-versus-voltage relations (Fig. 7B; recorded at the times indicated in panel A) and the 2-APB-sensitive component (difference current in Fig. 7C) show inward rectification, which was slightly less than with Ca^{2+} as the permeant ion, and no current reversal was seen. This is identical behavior to Orai1/CRAC channels under similar ionic conditions, owing to their low permeability to Cs^+ .⁵⁴ Lack of Cs^+ efflux also distinguishes Orai1/CRAC from TRPC channels, which are permeable to a wide

range of monovalent cations.^{55,56}

We exploited the large monovalent inward current carried by Na^+ (as in Fig. 7A–C) to examine the sensitivity of the store-operated current to three SOC inhibitors. The amplitude of the 2-APB-sensitive monovalent current at -110 mV was 4.4 ± 1.3 pA/pF ($n = 6$; 50 μM 2-APB), which was $55.3 \pm 2.4\%$ of the total monovalent current. The DES-sensitive component was 4.9 ± 1.9 pA/pF ($n = 5$; 10 μM DES), which was $56.1 \pm 5.2\%$ of the current. The SKF-96365-sensitive component was 4.4 ± 1.5 pA/pF ($n = 10$; 20 μM SKF-96365), $57.4 \pm 5.6\%$ of the current. The similarity in the amplitude and percent of current blocked by each of these SOC blockers provides evidence that the same channel underlies the SOCE seen with Fura-2 imaging and the store-operated current in whole-cell recordings in microglia.

The final experiments concerned the monovalent current that remained in the presence of SOC blockers. It is important to note that neither rundown nor hysteresis following exposure to DVF solution⁵⁷ reduced the current, and thus overestimated the block by 2-APB in Figure 7A. The amplitude of the remaining 2-APB insensitive monovalent current was the same (3.6 ± 1.1 pA/pF at -110 mV; $n = 3$) as in cells treated with 2-APB before the first exposure to DVF solution (i.e., 3.3 ± 1.4 pA/pF, $n = 8$; $p = 0.7558$). To verify that store depletion was necessary in order to elicit the 2-APB-sensitive current carried by Na^+ (Fig. 7C), we examined separate cells lacking depletion; i.e., without thapsigargin treatment and with an internal solution containing 100 nM free Ca^{2+} (see Materials and Methods). Under these conditions, the monovalent current in DVF solution (Fig. 7D) was quite variable (i.e., 3.0 ± 2.1 pA/pF, $n = 7$) but it did not exhibit a decay (unlike panel A) and was not sensitive to 50 μM 2-APB (i.e., it was reduced by 0.5 ± 0.3 pA/pF, $n = 3$). Thus, the remaining current was not the store-operated current described in Figure 7A. We next addressed the possibility that an inward-rectifying K^+ current could have produced the monovalent current in DVF bath

solutions. The rationale was that, under these culturing conditions, rat microglia have a prominent Kir, which is thought to be Kir2.1.^{24,47} Both this Kir current and cloned Kir2.1 channels are blocked by external divalent cations;^{24,47,58} thus, DVF solution might have reversed the channel block. Because Kir2.1 can be blocked by external Cs⁺,⁵⁹ we repeated the experiment from Figure 7A, but with 10 mM Cs⁺ added to the DVF solution. Exposure to DVF solution (Fig. 7E) evoked a large inward Na⁺ current, which rapidly decayed and was blocked by 10 μ M DES; the remaining current was 0.5 ± 0.2 pA/pF ($n = 3$; Fig. 7F). We could not find reports of Na⁺ permeability of Kir2.1 under the K⁺- and divalent-free conditions used here, but under normal conditions external Na⁺ blocks K⁺ influx at very negative potentials, causing a current relaxation. While our data support the possibility that Kir mediates the blocker-insensitive Na⁺ current, we cannot rule out an unidentified Cs⁺-sensitive current. We could not systematically test the SOC blockers on the remaining current because 10 mM external Cs⁺ reduced the recording stability.

Discussion

The broad importance of store-operated Ca²⁺ entry (SOCE) has generated considerable interest in identifying the underlying current. In microglia, SOCE occurs in response to activation of IP₃-linked metabotropic receptors: purinergic P₂Y,⁶⁰⁻⁶² C3a and C5a complement,⁶³ and platelet-activating factor.⁶⁴ Intracellular Ca²⁺ can also increase in response to chemokines, lipopolysaccharide (LPS), β -amyloid peptide, tumor necrosis factor- α , interleukin-1 β , interferon- γ , thrombin and lysophosphatidic acid.^{7,10,11,60,65} There are several candidates for the channel underlying SOCE, but insufficient pharmacological, biophysical and molecular information to distinguish among them. The cloning of TRP and Orai genes and evidence that Orai1 encodes the CRAC channel has provided useful new information that we have applied in this study. Thus, we quantified expression of several TRP and Orai genes in primary rat microglia, and then used patch-clamp and Fura-2 imaging methods to characterize the biophysical and pharmacological properties of a CRAC current that appears to account for the SOCE.

While numerous studies have addressed Ca²⁺ signaling in microglia (see Introduction), very few have attempted to identify the underlying currents. It can be difficult to separate the multiple Ca²⁺ currents that appear to be store dependent, and lack of consensus about which channel properties best discriminate among them has contributed to the confusion (reviewed in refs. 12 and 15). This is true for microglia as well, where TRPM7 was previously mistaken for Orai1/CRAC.^{51,54} Distinguishing Orai1/CRAC from some TRP channels requires extensive biophysical and pharmacological fingerprinting. Orai1/CRAC has an extremely small single-channel conductance (<0.2 pS), high selectivity for Ca²⁺ over monovalent cations ($P_{Ca}/P_{Na} > 1,000$), pronounced inward rectification with a very positive reversal potential, Ca²⁺-dependent current potentiation, and is blocked by SKF-96365, DES³⁵ and relatively high concentrations of 2-APB, but increased by low 2-APB concentrations.^{12,36} TRPM7 has a much larger conductance (~40 pS with Na⁺ as the permeant ion), is not store-dependent, and is pharmacologically distinct, with block by

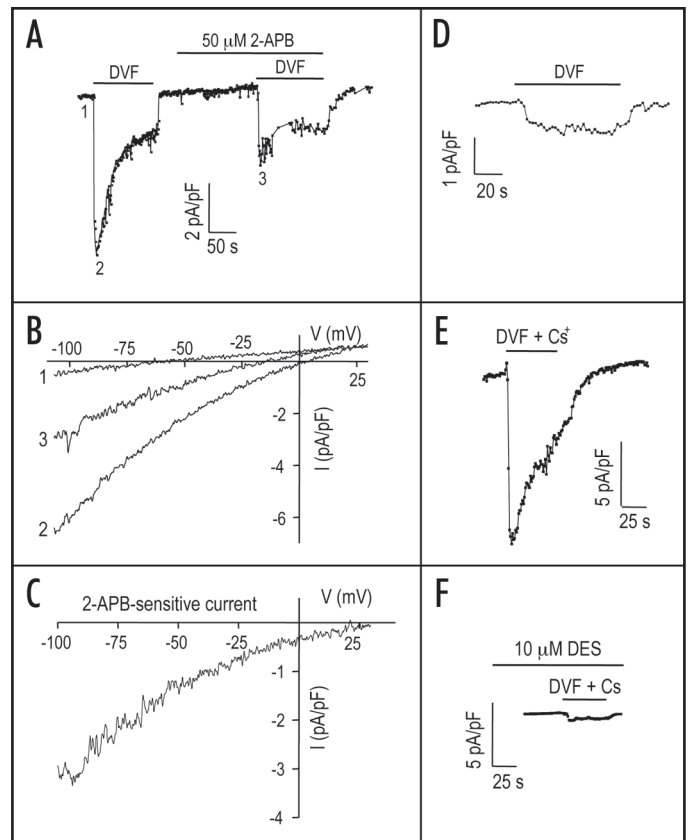


Figure 7. Ca²⁺-dependent potentiation and pharmacology of the store-operated current. As in Figure 5, microglia were incubated with 1 μ M thapsigargin (A–C, E and F): 5–7 min, standard bath solution) to deplete intracellular Ca²⁺ stores, and then exposed to K⁺ free solution. Current-versus-voltage (I-V) relations were continuously monitored by applying voltage ramps from -110 to +25 mV every 1 s from a holding potential of 0 mV. (A) Time course of the current amplitude monitored at -110 mV. The horizontal bars show periods when the bath contained divalent-free solution (DVF) rather than the normal Ca²⁺ and Mg²⁺ (1 mM each). Where indicated, 50 μ M 2-aminoethoxydiphenyl borate (2-APB) was included in the bath solution. (B) I-V relations taken from the cell in (A) at the numbered times; i.e., #1, K⁺-free bath solution with 1 mM Ca²⁺; #2, DVF bath solution; #3, DVF with 50 μ M 2-APB. (C) Isolation of the 2-APB-sensitive monovalent current using point-by-point subtraction of the current in trace #3 (DVF with 2-APB) from the current in trace #2 (DVF solution alone). (D) The same protocol and bath solutions as in (A), but applied to a microglial cell without store depletion (see text for conditions). (E and F) Two different microglial cells exposed to the same protocol as in (A), but using a DVF bath solution with 10 mM Cs⁺ alone (D) or in the presence of 10 μ M diethylstilbestrol (DES; E).

spermine and intracellular Mg²⁺, low sensitivity to SKF-96365 and 2-APB, and no block by DES (reviewed in refs. 12 and 15). Thus, the 42 pS current previously attributed to CRAC in rat microglia²² is likely mediated by TRPM7, which we characterized biophysically and pharmacologically in these cells.⁵⁰ TRPC1, TRPC3, TRPC6 and TRPC7 have been proposed as store-operated (reviewed in ref. 12) but they are less Ca²⁺ selective than Orai1/CRAC, with P_{Ca}/P_{Na} ratios of 1.6 for TRPC3,⁶⁶ ~5 for TRPC6,⁶⁷ and <0.4 for TRPC1.⁶⁸ Thus, one crucial test is to compare Ca²⁺-containing and divalent-free solutions.

Norenberg et al.²⁰ first showed that IP₃ in the pipette evoked an inwardly rectifying ('CRAC-like') Ca²⁺ current in rat microglia, which showed no reversal up to +100 mV. Other properties of the current were not examined and it was not related to store-operated Ca²⁺ entry; hence, it was important for us to extend that study using the most recent information about Orai1/CRAC. First, we identified a SOCE pathway that was entirely consistent with CRAC; i.e., inhibited by depolarization, and pharmacologically by Gd³⁺, SKF-96365, DES and 50 μM 2-APB (a relatively high concentration). Conversely, it was increased by hyper-polarization, by 5 μM 2-APB (a relatively low concentration), and exhibited Ca²⁺-dependent potentiation, which was not supported by Sr²⁺ or Ba²⁺. Then, we isolated a store-operated Ca²⁺ current and showed that its biophysical and pharmacological properties are entirely consistent with the currently known properties of cloned Orai1/CRAC channels; including activation by store depletion, high selectivity for Ca²⁺ over monovalent cations, pronounced inward rectification and a very positive reversal potential, Ca²⁺-dependent current potentiation, block by SKF-96365, DES or by 50 μM 2-APB. By assessing the properties of the store-operated Ca²⁺ entry and the Ca²⁺ current in the same cell type, this study strongly supports the contention that Orai1/CRAC channels produce the SOCE in microglia.

Physiological implications. In principle, SOCE and underlying Orai1/CRAC channels in microglia could affect numerous Ca²⁺-dependent molecules, including KCa channels,¹³ adenylyl cyclase, which raises cAMP,⁶⁹ phospholipase Cδ,⁷⁰ calmodulin and ionized calcium-binding adaptor molecule 1 (Iba-1). Studies are beginning to address whether the microglial activation state regulates SOCE and the expression/induction of the underlying currents. While it is anticipated that activity of Orai/CRAC channels will play a central role in microglial activation, there is very little information directly linking SOCE and CRAC currents. The biophysical and pharmacological evidence that SOCE can occur through an Orai/CRAC channel in microglia will be useful for future studies of Ca²⁺ signaling, and in discriminating its roles from other channels. One contribution of the present study was to establish conditions necessary to isolate and identify the small Orai/CRAC current carried by Ca²⁺ (~0.5 pA/pF) and the larger monovalent current in the absence of external Ca²⁺. The earliest studies of the currents lacked the necessary information to separate and identify CRAC currents, and would benefit from further investigation. For instance, the ability of LPS to activate SOCE in microglia⁷¹ and evoke a chronic Ca²⁺_i rise⁶⁰ suggests a sustained current activation, but an IP₃-activated 'CRAC' current was reportedly downregulated by LPS in murine microglia.²¹ Of note, in rat microglia, the current amplitude was an order of magnitude larger in LPS-activated cells²⁰ than in the unstimulated cells used in the present study.

In moving forward, it will be important to keep in mind that other non-selective cation currents have been seen in microglia. A non-rectifying current in rat microglia⁷² and human C13 cells⁷³ can be carried by Ca²⁺ (P_{Ca}/P_{Na} = 0.71) and shares some properties with cloned TRPM2 channels. It was activated by intracellular ADP-ribose, and by extracellular hydrogen peroxide, but only after LPS treatment in the rat microglia. In murine

microglia, a non-rectifying 'TRPM4-like' cation current (called 'I_{CAN}') was activated by micromolar levels of intracellular Ca²⁺, but was not affected by LPS.²¹ There might be species-dependent differences. We have not observed a Ca²⁺-activated I_{CAN} in rat microglia, despite testing a wide range of intracellular (pipette) Ca²⁺ concentrations (16 nM–40 μM, using both perforated- and conventional-patch clamp recordings), and assessing microglia in various activation states; i.e., ex vivo or cultured with serum-free medium, astrocyte-conditioned medium, LPS or phorbol ester.⁵⁰ Our present finding that TRPC1-TRPC7 are expressed in rat microglia raises the possibility of further Ca²⁺-permeable channels that might be dependent or independent of store depletion. Further channel complexity should be considered because of reports that TRPC and Orai1/CRAC channels co-assemble.^{74,75} However, most recent studies conclude that Orai1 forms homomultimers that co-assemble with the stromal interaction molecule 1 (STIM-1) protein,⁷⁶ and that TRPC1 and Orai1 produce separate currents.⁶⁸

We have demonstrated the conditions necessary for isolating the CRAC current from the numerous other currents that exist in rat microglia, and for comparing it with Ca²⁺-sensitive dye measurements of SOCE. This degree of characterization will be essential for clearly separating its contributions from identified TRP channels and for future studies of regulation of CRAC expression and activity. It is important to note that establishing roles for the CRAC current in microglia will require the development of a selective inhibitor. Microglia, like macrophages, are extremely resistant to siRNA-mediated knockdown, transfection and viral-mediated infection (we have carried out an exhaustive search for a molecular approach using >20 reagents/viral constructs). Thus, the only means to parse out Orai1/CRAC function is a pharmacological approach. Because the best available inhibitors, including SKF-96365, 2-APB and diethylstilbestrol, block other channels in addition to CRAC, it is not yet possible to assess its roles in assays of microglia function in vitro or in vivo.

Materials and Methods

Microglial cultures. All procedures were approved by the University Health Network animal care committee, in accordance with guidelines established by the Canadian Council on Animal Care. Microglia were isolated from brains of 1–2 day-old Wistar rats that had been killed by cervical dislocation. Cell cultures were prepared, as we have previously described.^{8,13,23,24} After carefully removing the meninges, whole brain tissue was mashed through a stainless steel sieve (100 mesh; Tissue Grinder Kit #CD-1; Sigma; Oakville, Canada), and then centrifuged (10 min, 1,000 g), re-suspended and seeded into flasks with MEM containing 10% fetal bovine serum (FBS) and 100 μM gentamycin (all from Invitrogen, Burlington, Canada). Two days later, cellular debris, non-adherent cells, and supernatant were removed and fresh medium was added to the flask. The mixed cultures were allowed to grow for 7–10 days and then shaken for 3 h on an orbital shaker at 8–10 Hz in a standard tissue culture incubator. The supernatant containing detached microglial cells was centrifuged (10 min, 1,000 g) and the cell pellet was re-suspended. Cells were

counted and plated at 3.5×10^4 cells per 15 mm diameter glass cover slip for electrophysiology or imaging. Before experiments, the plated microglia were cultured for 1–5 days in MEM with 100 μ M gentamycin, and a reduced serum concentration (2% FBS) to maintain a more resting state. This procedure yielded highly purified cultures of microglia (99–100%; see Fig. 1A), as judged by labeling with FITC-conjugated isolectin B4 or tomato lectin (both from Sigma, St. Louis, MO) or by immunofluorescence using the OX-42 monoclonal antibody (Serotec, Raleigh, NC), which recognizes complement receptor 3. We previously used quantitative real-time RT-PCR to demonstrate ~100% purity.¹³

Quantitative real-time reverse transcriptase polymerase chain reaction (qRT-PCR). Gene transcript levels were monitored in primary microglia ($\geq 99\%$ pure) using qRT-PCR,²⁵ as we recently described.^{8,13,26–28} Gene-specific primers (Table 1) were designed using the ‘Primer3Output’ program (http://frodo.wi.mit.edu/cgi-bin/primer3/primer3_www.cgi). RNeasy mini kits (Qiagen, Mississauga, ON) were used to isolate RNA after degrading any contaminating DNA with DNaseI (0.1 U/ml, 15 min, 37°C; Amersham Biosciences, PQ). A two-step reaction was performed according to the manufacturer’s instructions (Invitrogen). In brief, total RNA (1 μ g) was reverse transcribed in 20 μ l volume using 200 U of SuperScriptII RNase H-reverse transcriptase, with 0.5 mM dNTPs (Invitrogen) and 0.5 μ M oligo dT (Sigma). Amplification was performed on an ABI PRISM 7700 Sequence Detection System (PE Biosystems, Foster City, CA) at 95°C for 10 min, followed by 40 cycles at 95°C for 15 s, 56°C for 15 s and 72°C for 30 s. ‘No-template’ and ‘no-amplification’ controls were included for each gene, and melt curves showed a single peak, confirming specific amplification.²⁵ The threshold cycle (C_T) for each gene was determined and normalized against the housekeeping gene, hypoxanthine guanine phosphoribosyl transferase (HPRT1). The amplification efficiency was 90–95% for all the primers used.

Chemicals. Unless otherwise indicated, all chemicals including channel blockers were purchased from Sigma-Aldrich (Oakville, ON, Canada).

Single-cell fluorescence imaging. Microglia on cover slips were mounted in a perfusion chamber (Model RC-25, Warner Instruments, Hamden, CT) and the tissue culture medium was replaced with a bath solution containing (in mM): 135 NaCl, 5 KCl, 1 MgCl₂, 1 CaCl₂, 5 glucose and 10 HEPES, adjusted to pH 7.4 (with NaOH) and to ~300 mOsm with sucrose. For ion-substitution experiments, NaCl was partly or completely replaced with KCl, N-methyl-D-glucamine-chloride (NMDG-Cl) or LiCl, as indicated. For the nominally Ca²⁺-free solutions, CaCl₂ was omitted without adding EGTA, because we previously found that chelating all extracellular Ca²⁺ can evoke spontaneous Ca²⁺ depletion from immune cells.²⁹ This depletion compromises calibrating microglial Ca²⁺ levels from dye measurements. Images were acquired at room temperature using a Nikon Diaphot inverted microscope, Retiga-EX camera (Q-Imaging, Burnaby, BC, Canada), DG-4 arc lamp with excitation wavelength changer (Sutter Instruments, Novato, CA), and Northern Eclipse image acquisition software (Empix Imaging, Mississauga, ON, Canada).

Table 1 Sequences of primers used for quantitative RT-PCR analysis

Primer	Accession #	Sequence
HPRT1 (housekeeping)	NM_012583.2	F: CAGTACAGCCCCAAATGGT R: CAAGGGCATATCCAACAACA
TRPC1	NM_053558	F: GTGCTTGCGGCTTGAGAT R: TGCCATAGCTGGGGAAAC
TRPC2	NM_022638	F: ACGGCATCTTACCATCGTC R: GAGCGAGCAAACCTCCACTC
TRPC3	NM_021771	F: AGAGACACGGGCACAAGG R: GTTGGCAGTTGGGGTGAG
TRPC4	NM_053434	F: CGGTCCAGGCTCAACATC R: CTGAAAGCGGTGAGGAA
TRPC5	NM_080898	F: CAGAGGCAAAAGGTGAGGAG R: GTACAGGCAAAGGGATCAGG
TRPC6	AB051214	F: GCAGCAAGATGGGGAAGA R: GAGCAGCCCCAGGAAAAT
TRPC7	XM_225159	F: TCTCAGGCTTACGGCAACA R: ACGGAGCAATCCAATAGGC
TRPM2	NM_001011559.1	F: CCCCTACAAGCCCCAAGTGT R: GGCGAAGAGCAGGTAGAGG
TRPM7	XM_001056331	F: AGGGCAGTGGTTTGCTGT R: CAGGGCCAAAAACCATGT
Orai1	NM_001013982.1	F: GACTGGATCGGCCAGAGTT R: GAGAGCAGACGGGAGGTTTC
Orai2	XM_222288.4	F: CCGTGAGCAACATCCACA R: CAGCCAGGAAAAGCAGGA
Orai3	NM_001014024.1	F: CCACCAGTACCACACCA R: CCAGCCCACAAAAACAAC
CR3	NM_012711	F: TGCTGAGACTGGAGGCAAC R: CTCCCCAGCATCCTTGTTT
K _v 1.3	M30312	F: GCTCTCCCGCCATTCTAAG R: TCGTCTGCCTCAGCAAAGT

Images were acquired every 2–3 s, and the excitation shutter was closed between acquisitions to prevent photobleaching.

To measure intracellular Ca²⁺, microglia were loaded (~45 min, room temperature) with 3.5 μ g/ml Fura-2AM (Invitrogen, Burlington, ON, Canada) made in the indicated bath solution. Images were acquired at 340 and 380 nm excitation wavelengths, and ratios obtained using a 505 nm dichroic mirror and a 510 nm emission filter. In the representative figures, Fura-2 data are presented as the 340:380 nm ratio, and the summarized data in the text are presented as intracellular Ca²⁺ and Ba²⁺ levels, calibrated as previously described³⁰ using the values we determined for R_{\min} (0.25 ± 0.002) and R_{\max} (2.3 ± 0.097). Since we used 1 mM external Ca²⁺, while 2 mM is often used in studies on microglia, we compared the effects of 1 versus 2 mM external Ca²⁺. Resting intracellular Ca²⁺ was 70 ± 5 nM (56 cells) with 1 mM Ca²⁺ in the bath, 79 ± 5 nM after switching to 2 mM, and 85 ± 8 nM after returning to 1 mM ($p > 0.2$ for all comparisons). Hence, intracellular Ca²⁺ was well buffered against moderate changes in external Ca²⁺. For comparing Ca²⁺ and Ba²⁺ signals, the K_d values for

Table 2 Ionic composition of the bath solutions

Solution	NaCl	KCl	MgCl ₂	CaCl ₂	HEPES	D-glucose	EDTA	HEDTA ¹	NMDG-Cl	CsCl
1. Standard	130	5	1	1	10	5				
2. K free	135		1	1	10	5				
3. K free + Ca ²⁺	135		1	10	10	5				
4. DVF	135				10	5	1	10		
5. DVF + Cs ⁺	115	5			10	5				10
6. NMDG ⁺			3		10	5			135	
7. NMDG ⁺ + Ca ²⁺			1	20	10	5			108	

¹*N*-(2-Hydroxyethyl)ethylenediamine-*N,N'*-triacetic acid.

intracellular Fura-2 binding were taken as 236 nM for Ca²⁺,^{31,32} and 780 nM for Ba²⁺.³²

Patch clamp recordings. Conventional whole-cell recordings were made at room temperature with pipettes (2–5 MΩ resistance) pulled from borosilicate glass (WPI, Sarasota, FL). Recordings were made with either an Axon multiclamp 700A or an Axopatch 200 amplifier (Molecular Devices, Sunnyvale, CA), compensated on-line for capacitance and series resistance, and filtered at 5 kHz. Patch-clamp data were acquired and digitized using a Digidata 1322A board with pCLAMP software (version 9.2, Molecular Devices), and analyzed using Origin ver7.0 software (OriginLabs, Northampton, MA). Liquid-liquid junction potentials were calculated using the utility in pCLAMP, confirmed using a 3 M KCl electrode,³³ and subtracted before data analysis. Standard intracellular (pipette) solution contained (in mM): 100 K aspartate, 40 KCl, 1 MgCl₂, 1 CaCl₂, 10 EGTA (20 nM free Ca²⁺), 10 HEPES, 2 MgATP. The pH of all pipette solutions was adjusted to 7.2 with KOH. The high buffering-capacity pipette solution used for isolating the CRAC current contained (in mM) 125 Cs-aspartate, 8 MgCl₂, 10 BAPTA, 10 HEPES. The low buffering-capacity pipette solution contained (mM) 125 Cs-aspartate, 8 MgCl₂, 0.475 CaCl₂, 1 BAPTA (100 nM free Ca²⁺), 10 HEPES. Table 2 shows the composition of all extracellular solutions, which were adjusted to pH 7.4 with NaOH. The osmolarity of all recording solutions was adjusted to 290–310 mOsm by adding sucrose.

In a subset of recordings, the voltage dependence of Ca²⁺ entry was assessed by combining Ca²⁺ imaging with perforated patch-clamp recordings. In this case, microglial cells were labeled with Fura-2AM as described above, and the pipette solution contained 200 μM amphotericin (Sigma) diluted from a stock solution made in DMSO. After obtaining a giga-ohm seal, amphotericin caused a gradual decrease in series resistance, and when it reached <100 MΩ, experiments were begun.

Unless otherwise is stated, all quantitative data are presented as the mean ± SD. For clarity, statistical tests are described with each result.

Acknowledgements

Part of this work was published as an abstract; Evan W. Newell and Lyne C. Schlichter, Abstract 845.17 Society for Neuroscience Annual Meeting, Washington, Nov. 2005. We thank

Xiaoping Zhu for conducting the real-time RT-PCR analysis and Guillaume Ducharme for helpful discussions. This work was supported by grants to Lyne C. Schlichter from the Canadian Institutes for Health Research (CIHR; #MT-13657) and the Heart and Stroke Foundation, Ontario chapter (#T4670), and a grant to Elise F. Stanley (CIHR; MOP-86643). Evan W. Newell was supported by a Ruth L. Kirschstein National Research Service Award pre-doctoral scholarship from the National Institutes of Neurological Diseases and Stroke (#F31NS049742).

References

- Inoue K, Nakajima K, Morimoto T, Kikuchi Y, Koizumi S, Illes P, Kohsaka S. ATP stimulation of Ca²⁺-dependent plasminogen release from cultured microglia. *Br J Pharmacol* 1998; 123:1304-10.
- McLarnon JG, Wang X, Bae JH, Kim SU. Endothelin-induced changes in intracellular calcium in human microglia. *Neurosci Lett* 1999; 263:9-12.
- Morigiwa K, Quan M, Murakami M, Yamashita M, Fukuda Y. P2 Purinoreceptor expression and functional changes of hypoxia-activated cultured rat retinal microglia. *Neurosci Lett* 2000; 282:153-6.
- Moller T, Contos JJ, Musante DB, Chun J, Ransom BR. Expression and function of lysophosphatidic acid receptors in cultured rodent microglial cells. *J Biol Chem* 2001; 276:25946-52.
- D'Aversa TG, Yu KO, Berman JW. Expression of chemokines by human fetal microglia after treatment with the human immunodeficiency virus type 1 protein Tat. *J Neurovirol* 2004; 10:86-97.
- Moller T, Kann O, Verkhratsky A, Kettenmann H. Activation of mouse microglial cells affects P2 receptor signaling. *Brain Res* 2000; 853:49-59.
- Farber K, Kettenmann H. Functional role of calcium signals for microglial function. *Glia* 2006; 54:656-65.
- Newell EW, Stanley EF, Schlichter LC. Reversed Na⁺/Ca²⁺ exchange contributes to Ca²⁺ influx and respiratory burst in microglia. *Channels (Austin)* 2007; 1:366-76.
- Eder C. Regulation of microglial behavior by ion channel activity. *J Neurosci Res* 2005; 81:314-21.
- Moller T. Calcium signaling in microglial cells. *Glia* 2002; 40:184-94.
- Farber K, Kettenmann H. Purinergic signaling and microglia. *Pflügers Arch* 2006; 452:615-21.
- Parekh AB, Putney JW Jr. Store-operated calcium channels. *Physiol Rev* 2005; 85:757-810.
- Kaushal V, Koeberle PD, Wang Y, Schlichter LC. The Ca²⁺-activated K⁺ channel KCNN4/KCa3.1 contributes to microglia activation and nitric oxide-dependent neurodegeneration. *J Neurosci* 2007; 27:234-44.
- Hoth M, Penner R. Calcium release-activated calcium current in rat mast cells. *J Physiol* 1993; 465:359-86.
- Prakriya M, Lewis RS. CRAC channels: activation, permeation, and the search for a molecular identity. *Cell Calcium* 2003; 33:311-21.
- Feske S, Gwack Y, Prakriya M, Srikanth S, Puppel SH, Tanasa B, et al. A mutation in Orai1 causes immune deficiency by abrogating CRAC channel function. *Nature* 2006; 441:179-85.
- Vig M, Peinelt C, Beck A, Koomoa DL, Rabah D, Koblan-Huberson M, et al. CRACM1 is a plasma membrane protein essential for store-operated Ca²⁺ entry. *Science* 2006; 312:1220-3.

18. Yeromin AV, Zhang SL, Jiang W, Yu Y, Safrina O, Cahalan MD. Molecular identification of the CRAC channel by altered ion selectivity in a mutant of Orai. *Nature* 2006; 443:226-9.
19. Prakriya M, Feske S, Gwack Y, Srikanth S, Rao A, Hogan PG. Orai1 is an essential pore subunit of the CRAC channel. *Nature* 2006; 443:230-3.
20. Norenberg W, Cordes A, Blohbaum G, Frohlich R, Illes P. Coexistence of purino- and pyrimidinocceptors on activated rat microglial cells. *Br J Pharmacol* 1997; 121:1087-98.
21. Beck A, Penner R, Fleig A. Lipopolysaccharide-induced downregulation of Ca²⁺ release-activated Ca²⁺ currents (I_{CRAC}) but not Ca²⁺-activated TRPM4-like currents (I_{CAN}) in cultured mouse microglial cells. *J Physiol* 2008; 586:427-39.
22. Hahn J, Jung W, Kim N, Uhm DY, Chung S. Characterization and regulation of rat microglial Ca²⁺ release-activated Ca²⁺ (CRAC) channel by protein kinases. *Glia* 2000; 31:118-24.
23. Fordyce CB, Jagasia R, Zhu X, Schlichter LC. Microglia K_v1.3 channels contribute to their ability to kill neurons. *J Neurosci* 2005; 25:7139-49.
24. Newell EW, Schlichter LC. Integration of K⁺ and Cl⁻ currents regulate steady-state and dynamic membrane potentials in cultured rat microglia. *J Physiol* 2005; 567:869-90.
25. Bustin SA, Nolan T. Pitfalls of quantitative real-time reverse-transcription polymerase chain reaction. *J Biomol Tech* 2004; 15:155-66.
26. Ducharme G, Newell EW, Pinto C, Schlichter LC. Small-conductance Cl⁻ channels contribute to volume regulation and phagocytosis in microglia. *Eur J Neurosci* 2007; 26:2119-30.
27. Wasserman JK, Zhu X, Schlichter LC. Evolution of the inflammatory response in the brain following intracerebral hemorrhage and effects of delayed minocycline treatment. *Brain Res* 2007; 1180:140-54.
28. Wasserman JK, Schlichter LC. Neuron death and inflammation in a rat model of intracerebral hemorrhage: effects of delayed minocycline treatment. *Brain Res* 2007; 1136:208-18.
29. Schlichter LC, Sakellaropoulos G. Intracellular Ca²⁺ signaling induced by osmotic shock in human T lymphocytes. *Exp Cell Res* 1994; 215:211-22.
30. Gryniewicz G, Poenie M, Tsien RY. A new generation of Ca²⁺ indicators with greatly improved fluorescence properties. *J Biol Chem* 1985; 260:3440-50.
31. Fanger CM, Neben AL, Cahalan MD. Differential Ca²⁺ influx, K_{Ca} channel activity, and Ca²⁺ clearance distinguish Th1 and Th2 lymphocytes. *J Immunol* 2000; 164:1153-60.
32. Schilling WP, Rajan L, Strobl-Jager E. Characterization of the bradykinin-stimulated calcium influx pathway of cultured vascular endothelial cells. Saturability, selectivity and kinetics. *J Biol Chem* 1989; 264:12838-48.
33. Barry PH, Lynch JW. Liquid junction potentials and small cell effects in patch-clamp analysis. *The Journal of membrane biology* 1991; 121:101-17.
34. Kotecha SA, Schlichter LC. A K_v1.5 to K_v1.3 switch in endogenous hippocampal microglia and a role in proliferation. *J Neurosci* 1999; 19:10680-93.
35. Zakharov SI, Smani T, Dobrydneva Y, Monje F, Fichandler C, Blackmore PF, Bolotina VM. Diethylstilbestrol is a potent inhibitor of store-operated channels and capacitative Ca²⁺ influx. *Mol Pharmacol* 2004; 66:702-7.
36. Peinelt C, Lis A, Beck A, Fleig A, Penner R. 2-Aminoethoxydiphenyl borate directly facilitates and indirectly inhibits STIM1-dependent gating of CRAC channels. *J Physiol* 2008; 586:3061-73.
37. Rae J, Cooper K, Gates P, Watsky M. Low access resistance perforated patch recordings using amphotericin B. *J Neurosci Methods* 1991; 37:15-26.
38. Zweifach A, Lewis RS. Slow calcium-dependent inactivation of depletion-activated calcium current. Store-dependent and -independent mechanisms. *J Biol Chem* 1995; 270:14445-51.
39. Christian EP, Spence KT, Togo JA, Dargis PG, Patel J. Calcium-dependent enhancement of depletion-activated calcium current in Jurkat T lymphocytes. *J Membr Biol* 1996; 150:63-71.
40. Sinkins WG, Estacion M, Schilling WP. Functional expression of TrpC1: a human homologue of the *Drosophila* Trp channel. *Biochem J* 1998; 331:331-9.
41. Zhang L, Saffen D. Muscarinic acetylcholine receptor regulation of TRP6 Ca²⁺ channel isoforms. Molecular structures and functional characterization. *J Biol Chem* 2001; 276:13331-9.
42. Philipp S, Strauss B, Hirnet D, Wissenbach U, Mery L, Flockerzi V, Hoth M. TRPC3 mediates T-cell receptor-dependent calcium entry in human T-lymphocytes. *J Biol Chem* 2003; 278:26629-38.
43. Venkatachalam K, Zheng F, Gill DL. Control of TRPC and store-operated channels by protein kinase C. *Novartis Found Symp* 2004; 258:172-85.
44. Grimaldi M, Maratos M, Verma A. Transient receptor potential channel activation causes a novel form of [Ca²⁺]_i oscillations and is not involved in capacitative Ca²⁺ entry in glial cells. *J Neurosci* 2003; 23:4737-45.
45. North RA. Molecular physiology of P2X receptors. *Physiol Rev* 2002; 82:1013-67.
46. Zweifach A, Lewis RS. Calcium-dependent potentiation of store-operated calcium channels in T lymphocytes. *J Gen Physiol* 1996; 107:597-610.
47. Schlichter LC, Sakellaropoulos G, Ballyk B, Pennefather PS, Phipps DJ. Properties of K⁺ and Cl⁻ channels and their involvement in proliferation of rat microglial cells. *Glia* 1996; 17:225-36.
48. Cayabyab FS, Schlichter LC. Regulation of an ERG K⁺ current by Src tyrosine kinase. *J Biol Chem* 2002; 277:13673-81.
49. Cayabyab FS, Tsui FW, Schlichter LC. Modulation of the ERG K⁺ current by the tyrosine phosphatase, SHP-1. *J Biol Chem* 2002; 277:48130-8.
50. Jiang X, Newell EW, Schlichter LC. Regulation of a TRPM7-like current in rat brain microglia. *J Biol Chem* 2003; 278:42867-76.
51. Kozak JA, Kerschbaum HH, Cahalan MD. Distinct properties of CRAC and MIC channels in RBL cells. *J Gen Physiol* 2002; 120:221-35.
52. Cahalan MD, Zhang SL, Yeromin AV, Ohlsen K, Roos J, Stauderman KA. Molecular basis of the CRAC channel. *Cell Calcium* 2007; 42:133-44.
53. Lepple-Wienhues A, Cahalan MD. Conductance and permeation of monovalent cations through depletion-activated Ca²⁺ channels (I_{CRAC}) in Jurkat T cells. *Biophys J* 1996; 71:787-94.
54. Prakriya M, Lewis RS. Separation and characterization of currents through store-operated CRAC channels and Mg²⁺-inhibited cation (MIC) channels. *J Gen Physiol* 2002; 119:487-507.
55. Zitt C, Obukhov AG, Strubing C, Zobel A, Kalkbrenner F, Luckhoff A, Schultz G. Expression of TRPC3 in Chinese hamster ovary cells results in calcium-activated cation currents not related to store depletion. *J Cell Biol* 1997; 138:1333-41.
56. Lintschinger B, Balzer-Geldsetzer M, Baskaran T, Graier WF, Romanin C, Zhu MX, Groschner K. Coassembly of Trp1 and Trp3 proteins generates diacylglycerol- and Ca²⁺-sensitive cation channels. *J Biol Chem* 2000; 275:27799-805.
57. Prakriya M, Lewis RS. Regulation of CRAC channel activity by recruitment of silent channels to a high open-probability gating mode. *J Gen Physiol* 2006; 128:373-86.
58. Owen JM, Quinn CC, Leach R, Findlay JB, Boyett MR. Effect of extracellular cations on the inward rectifying K⁺ channels Kir2.1 and Kir3.1/Kir3.4. *Exp Physiol* 1999; 84:471-88.
59. Thompson GA, Leyland ML, Ashmole I, Sutcliffe MJ, Stanfield PR. Residues beyond the selectivity filter of the K⁺ channel kir2.1 regulate permeation and block by external Rb⁺ and Cs⁺. *J Physiol* 2000; 526:231-40.
60. Hoffmann A, Kann O, Ohlemeyer C, Hanisch UK, Kettenmann H. Elevation of basal intracellular calcium as a central element in the activation of brain macrophages (microglia): suppression of receptor-evoked calcium signaling and control of release function. *J Neurosci* 2003; 23:4410-9.
61. Choi HB, Hong SH, Ryu JK, Kim SU, McLarnon JG. Differential activation of subtype purinergic receptors modulates Ca²⁺ mobilization and COX-2 in human microglia. *Glia* 2003; 43:95-103.
62. Toescu EC, Moller T, Kettenmann H, Verkhratsky A. Long-term activation of capacitative Ca²⁺ entry in mouse microglial cells. *Neuroscience* 1998; 86:925-35.
63. Moller T, Nolte C, Burger R, Verkhratsky A, Kettenmann H. Mechanisms of C5a and C3a complement fragment-induced [Ca²⁺]_i signaling in mouse microglia. *J Neurosci* 1997; 17:615-24.
64. Wang X, Bae JH, Kim SU, McLarnon JG. Platelet-activating factor induced Ca²⁺ signaling in human microglia. *Brain Res* 1999; 842:159-65.
65. McLarnon JG. Purinergic mediated changes in Ca²⁺ mobilization and functional responses in microglia: effects of low levels of ATP. *J Neurosci Res* 2005; 81:349-56.
66. Kamouchi M, Philipp S, Flockerzi V, Wissenbach U, Mamin A, Raeymaekers L, et al. Properties of heterologously expressed hTRP3 channels in bovine pulmonary artery endothelial cells. *J Physiol* 1999; 518:345-58.
67. Hofmann T, Obukhov AG, Schaefer M, Harteneck C, Gudermann T, Schultz G. Direct activation of human TRPC6 and TRPC3 channels by diacylglycerol. *Nature* 1999; 397:259-63.
68. Zarayskiy V, Monje F, Peter K, Csutora P, Khodorov BI, Bolotina VM. Store-operated Orai1 and IP3 receptor-operated TRPC1 channel. *Channels (Austin)* 2007; 1:246-52.
69. Cooper DM, Karpen JW, Fagan KA, Mons NE. Ca²⁺-sensitive adenylyl cyclases. *Adv Second Messenger Phosphoprotein Res* 1998; 32:23-51.
70. Kim YH, Park TJ, Lee YH, Baek KJ, Suh PG, Ryu SH, Kim KT. Phospholipase C-delta1 is activated by capacitative calcium entry that follows phospholipase C-beta activation upon bradykinin stimulation. *J Biol Chem* 1999; 274:26127-34.
71. Bader MF, Taupenot L, Ulrich G, Aunis D, Ciesielski-Treska J. Bacterial endotoxin induces [Ca²⁺]_i transients and changes the organization of actin in microglia. *Glia* 1994; 11:336-44.
72. Kraft R, Grimm C, Grosse K, Hoffmann A, Sauerbruch S, Kettenmann H, et al. Hydrogen peroxide and ADP-ribose induce TRPM2-mediated calcium influx and cation currents in microglia. *Am J Physiol Cell Physiol* 2004; 286:129-37.
73. Fonfria E, Mattei C, Hill K, Brown JT, Randall A, Benham CD, et al. TRPM2 is elevated in the tMCAO stroke model, transcriptionally regulated and functionally expressed in C13 microglia. *J Recept Signal Transduct Res* 2006; 26:179-98.
74. Liao Y, Exrleben C, Abramowitz J, Flockerzi V, Zhu MX, Armstrong DL, Birnbaumer L. Functional interactions among Orai1, TRPCs and STIM1 suggest a STIM-regulated heteromeric Orai/TRPC model for SOCE/Icrac channels. *Proc Natl Acad Sci USA* 2008; 105:2895-900.
75. Redondo PC, Jardin I, Lopez JJ, Salido GM, Rosado JA. Intracellular Ca²⁺ store depletion induces the formation of macromolecular complexes involving hTRPC1, hTRPC6, the type II IP3 receptor and SERCA3 in human platelets. *Biochim Biophys Acta* 2008; 1783:1163-76.
76. Lewis RS. The molecular choreography of a store-operated calcium channel. *Nature* 2007; 446:284-7.